https://doi.org/10.3311/PPci.41452



**Periodica Polytechnica Civil Engineering**, 69(4), pp. 1333–1344, 2025

# Behavior of Flat Slabs with Partial Use of SIFCON Subjected to Concentrated Loading

Wisam K. Tuama[1*], György László Balázs[1]

[1] Department of Construction Materials and Technologies, Faculty of Civil Engineering, Budapest University of Technology and Economics, Műegyetem rkp. 3., H-1111 Budapest, Hungary
[*] Corresponding author, e-mail: wisamkamiltuamaalzweehm@edu.bme.hu

Received: 28 June 2025, Accepted: 24 October 2025, Published online: 10 November 2025

**Abstract**

This research investigates the applicability of slurry-infiltrated fiber concrete (SIFCON) to enhance ductility and punching shear capacity. In addition, especially since the SIFCON mortar is considered self-compacting, thus reduces the labor costs associated with concrete vibration. Eight flat slabs with dimension 600 × 600 × 60 mm, were cast and tested under concentrated loading. The main experimental parameters investigated were the type of concrete (NSC and SIFCON), the placement of SIFCON within the slab, and the proportion of the slab area composed of SIFCON. Among the tested specimens, one slab was constructed entirely with NSC and another entirely with SIFCON; these two slabs served as reference specimens for comparative evaluation. The experimental results are presented, including maximum load, deflection, ductility, and rotation, as well as the crack pattern of each specimen and the inclination of cracks. According to the test results, punching shear of RC slabs and deformation capacities are considerably increased by using SIFCON. The percentage increase in punching shear capacity of the slab with SIFCON layer 40 mm in the tension face was 112%, and the ductility of the slab with SIFCON layer 20 mm in the tension face was 117%, compared with the reference slab. Furthermore, by increasing the post-punching deformations of slabs, the strengthening approach may also be applied to prevent structures from collapsing suddenly following punching shear failure.

**Keywords**

flat slab, slurry infiltrated fiber concrete, punching shear, RC-SIFCON, steel fibers

## 1 Introduction

Reinforced concrete (RC) flat slabs are widely used in multistory buildings around the world. The design is often governed by punching shear and serviceability in these slabs. minimizing these difficulties during the design process typically results in increased raw material usage and expenses. Previous research has shown that using fiber-reinforced concrete (FRC), high-strength concrete (HSC), or other special concretes only near the column, while casting the rest of the slab with normal strength concrete (NSC), can result in better behavior under gravity loads in terms of serviceability and ultimate capacity [1].

There is the worry that brittle punching shear failure will occur in flat slabs around columns. Several strategies have been proposed to improve the punching shear capacity of flat slabs constructed with NSC. The methods include increasing the slab thickness, utilizing column heads, using drop panels, providing extra shear reinforcement, and deploying new materials, such as fiber-reinforced polymer (FRP) [2–4].

Because the expense and complexity of the previously stated procedures could reduce the primary advantages of flat slabs in some scenarios, improved strategies to boost punching shear capacity must be researched. The punching shear behavior of UHPFRC slabs with varying concrete compressive strengths, flexural reinforcement kinds and percentages, steel fibers, and column aspect ratios was studied. The fiber volume was limited to no more than 2%. These testing findings showed that using UHPFRC in slabs considerably increased punching shear strength and ductility compared to NSC or HSC slabs. Furthermore, fiber composition (volume, kind, size, shape, etc.) had a significant impact on punching shear strength and slab ductility [5]. Steel FRC is considered an option in these situations to improve the flat slab's performance, punching shear

**Cite this article as:** Tuama, W. K., Balázs, G. L. "Behavior of Flat Slabs with Partial Use of SIFCON Subjected to Concentrated Loading", Periodica Polytechnica Civil Engineering, 69(4), pp. 1333–1344, 2025. https://doi.org/10.3311/PPci.41452

capacity, and cracking management. A sufficient quantity of steel fiber has demonstrated its capacity to offer an effective reinforcing mechanism through its bridging action, hence improving the flat slab's stability [6, 7].

Slurry infiltrated fiber concrete (SIFCON) is a steel fiber-reinforced cement composite with outstanding toughness as well as excellent mechanical qualities such as compressive, tensile, shear, and flexural strength [8]. SIFCON demonstrated markedly superior energy-absorption capacity relative to conventional FRC and other specialized concretes [9]. Fiber composition of SIFCON by volume ranges from 4 to 20%. This ratio typically does not exceed 2% in traditional FRC due to workability and mixing requirements, where the fibers are mixed with the other ingredients of the concrete: cement, sand, and gravel. As for SIFCON concrete, its production method is different. A high quantity of fibers is placed in the mold, and then mortar is poured into the space between the fibers.

Very limited research is on the optimal application of SIFCON to strengthening the critical area of flat slab exists in the literature. In this study, the RC-SIFCON flat slab specimens, i.e., RC flat slab with local SIFCON inserts to increase punching resistance, were used to identify the extent of the effect of using SIFCON as a part of reinforced NSC flat slab on punching shear resistance.

## 2 Experimental work

### 2.1 Materials and mix design

In the field of this study, the mix composition of SIFCON and NC used is indicated in Table 1. Normal quartz sand with 0.4–1 and 1–4 mm size used as a fine aggregate for SIFCON and NSC, respectively. 4–8 and 8–16 mm used as a coarse aggregate for NSC. Portland cement type CEM I (42.5), and silica fume conforming with ASTM C1240-15 standard [10] used as a binder. 50% and 30% used as a water to cementitious materials ratio (w/c) for NSC and SIFCON respectively. BASF Master Glenium 300 as a superplasticizer with 1.75% used in the SIFCON mixture to set the consistency of concrete flow [11]. The flexural reinforcements of RC slabs were designed using ACI 318-19 standard [12]. To ensure the failure mode of slabs in punching shear, the flat concrete slab should be reinforced with adequate flexural reinforcement to prevent flexural failure, one size of deformed steel bars was used as main reinforcing bars with size of Ø 10 mm nominal diameter with yield strength is equal to 500 MPa used as flexural reinforcement placed in the tension face of flat slabs. In this work, hooked-end steel fibers 6% are used with a length of 35 mm and a diameter of 0.6 mm with an aspect ratio of about 58. Fig. 1 displays the fiber used in this research. Table 2 indicates the technical properties of the fiber used according to the manufacturer company.

Fig. 2 shows the materials proportion used in NSC and SIFCON mixture as a percentage of total mix weight. The fiber volume fraction utilized in this investigational work was 6% because it was the suitable fiber volume of the molds. Fig. 3 describes the SIFCON mix technique used in this study, which was based on prior research and trial mixtures to get suitable workability.

**Table 1** NSC and SIFCON optimal mixing proportions for 1 m³

| Materials | NSC | SIFCON |
|---|---|---|
| Cement (kg/m³) | 370 | 873 |
| Sand (0.4–1) mm (kg/m³) | – | 970 |
| Sand (1–4) mm (kg/m³) | 924 | – |
| Coarse agg. (4–16) mm (kg/m³) | 924 | – |
| Silica fume 10% rep. (kg/m³) | – | 97 |
| Steel fiber (%) | – | 6 |
| w/b or w/c ratio (%) | 50 | 30 |
| SP (by wt. of binder) (%) | – | 1.75 |

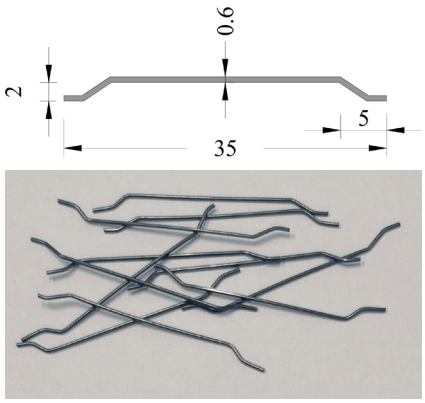


**Fig. 1** Hooked-end steel fiber (the dimensions are millimeters)

**Table 2** NSC and SIFCON optimal mixing proportions for 1 m³

| Length (mm) | Diameter (mm) | Aspect ratio (l/d) | Density (kg/m³) | Tensile strength (MPa) |
|---|---|---|---|---|
| 35 ± 5% | 0.6 ± 5% | 58 | 7,850 | 1,350 |

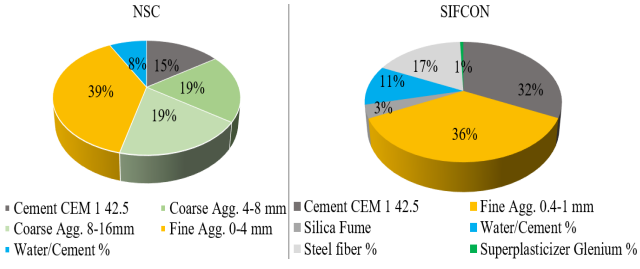


**Fig. 2** Materials proportion used in NSC and SIFCON mixture (% of total mix weight)

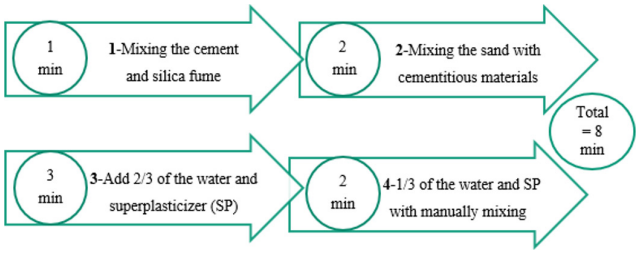


**Fig. 3** The SIFCON mix technique used in this study

The procedure of SIFCON mixing: Blend the dry material for 3 min; after that, add 2/3 of water that was mixed with Superplasticizer for 3 min; then add the remaining amount of 1/3 water with superplasticizer and continue mixing for 2 min. The workability of slurry was achieved with an extent diameter in this test of 260 mm which is performed using the flow test (ASTM C1437-15 standard [13]).

### 2.2 Casting and testing samples and specimens

This study contained compressive and flexural strength tests on NSC and SIFCON. Compressive strength was investigated using 150 and 100 mm cubes for NSC and SIFCON, respectively. Flexural strength tests were conducted on prisms measuring 700 × 700 × 250, and 40 × 40 × 160 mm for NSC and SIFCON respectively. The results are the average of three cubes or prisms for all sets at the ages of 7 and 28 days.

The main objective of this study is to examine the structural behavior of RC flat slabs with partial use of SIFCON. The experimental program consisted of testing 8 slab specimens, two reference specimens were cast, one NSC and the other SIFCON. 6 RC-SIFCON composite flat slab specimens cast and compared with the references. Each test slab of the present investigation was a square slab with a full side length of 600 mm with thicknesses of 60 mm. Slab specimens were divided into three groups depending on the location of SIFCON in the NSC flat slab as shown in Table 3. Fig. 4 shows the symbol of slab specimen.

In this study, we chose the area of SIFCON zone depending on the ACI 318-19 standard [12], it indicates that the critical perimeter of the punching shear, should not be less than d/2 from a column's four faces and the Eurocode 2 [14] specifies that the control perimeter extends a distance of 2d from the four faces of a column, where d is the average effective depth of the reinforcement. Therefore, a more considerable distance equal to the thickness of the slab was used from the face of the loading area in each direction to ensure coverage of the entire critical area. The minimum and maximum distances for the area of the SIFCON zone were 180 mm$^2$ and 300 mm$^2$. Fig. 5 [12, 13] presents

**Table 3** The symbols of slab and their meanings

| No. of Group | Symbol | Details | Dimensions of SIFCON (mm) |
|---|---|---|---|
| Group 1 | N | NSC | – |
| | S | SIFCON | 600 × 600 × 60 |
| Group 2 | N-ST60-2 | NSC-SIFCON in tension face | 600 × 600 × 20 |
| | N-ST60-4 | NSC-SIFCON in tension face | 600 × 600 × 40 |
| Group 3 | N-SC18-2 | NSC-SIFCON in center of tension face | 180 × 180 × 20 |
| | N-SC18-4 | NSC-SIFCON in center of tension face | 180 × 180 × 40 |
| | N-SC18-6 | NSC-SIFCON in the center | 180 × 180 × 60 |
| | N-SC30-6 | NSC-SIFCON in the center | 300 × 300 × 60 |

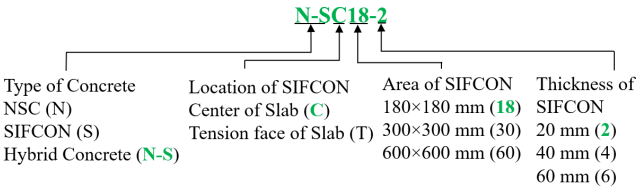


**Fig. 4** An instance for the method used to identify slab specimens

the control perimeters of slabs without shear reinforcement specified by both codes. Fig. 6 shows the overall slab geometries and reinforcement layout details.

Before starting the process of casting the slab specimens, the selected materials were prepared and weighed according to the volume of the mix. All slabs test specimens used in this research were cast in wooden molds on the sides, resting on an iron floor and surrounded by iron outer sides to provide sufficient support for measuring with dimensions of 600 × 600 × 60 mm.

Before casting, the molds were cleaned and lubricated before each casting and placed on the horizontal ground.

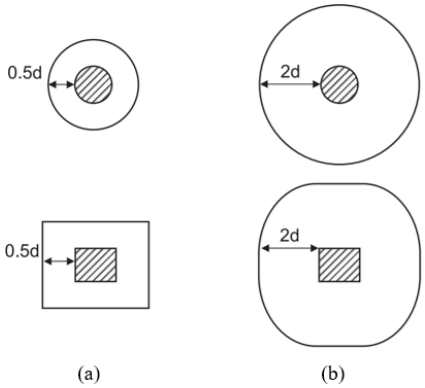


**Fig. 5** The perimeters of slabs without shear reinforcement specified by codes: (a) Critical perimeter per ACI 318-19 (d/2) [12]; (b) Control perimeter per Eurocode 2 (2d) [13]

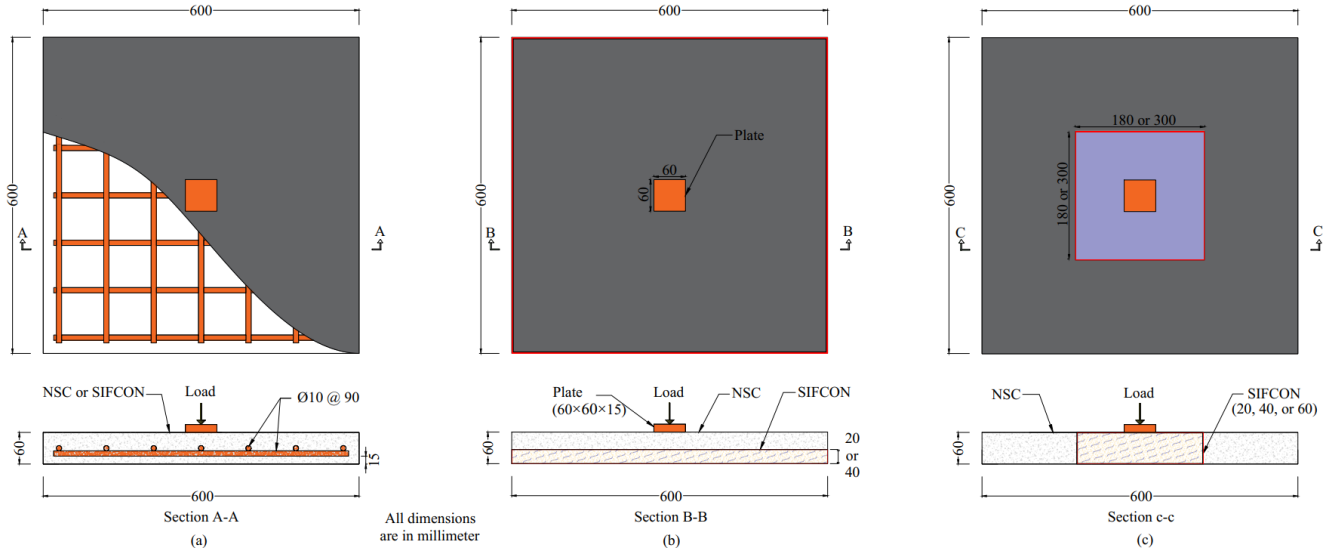


**Fig. 6** Specimen dimensions and layout: (a) Group 1 and reinforcement details; (b) Group 2; (c) Group 3

Fig. 7 shows the steps of casting the different types of concrete in this study. For NSC, the reinforcement mesh was positioned carefully inside the mold with the required bottom cover being accurately maintained, for SIFCON flat slab, in addition to placing the reinforcement mesh, the fiber amount was put at once before pouring the slurry to penetrate the fibers. For RC-SIFCON, a fine galvanized steel mesh was positioned at the interface between the NSC and SIFCON zones, anchored to the bottom reinforcement and supported by wooden formwork from above to maintain precise dimensions, as shown in the same Fig. 7. Due to the self-compacting behavior and relatively rapid setting of SIFCON, the outer region was cast first using NSC, followed shortly by the placement of SIFCON in the inner zone. After the mixing was finished, the fresh NSC or SIFCON mixture was poured into the molds. Slab specimens were cured with saturated wet coverings, while samples were cured in a water tank with a temperature of 23 ± 2 °C.

All of the slab specimens were tested at the age of 28 days under increasing concentric load up to failure by

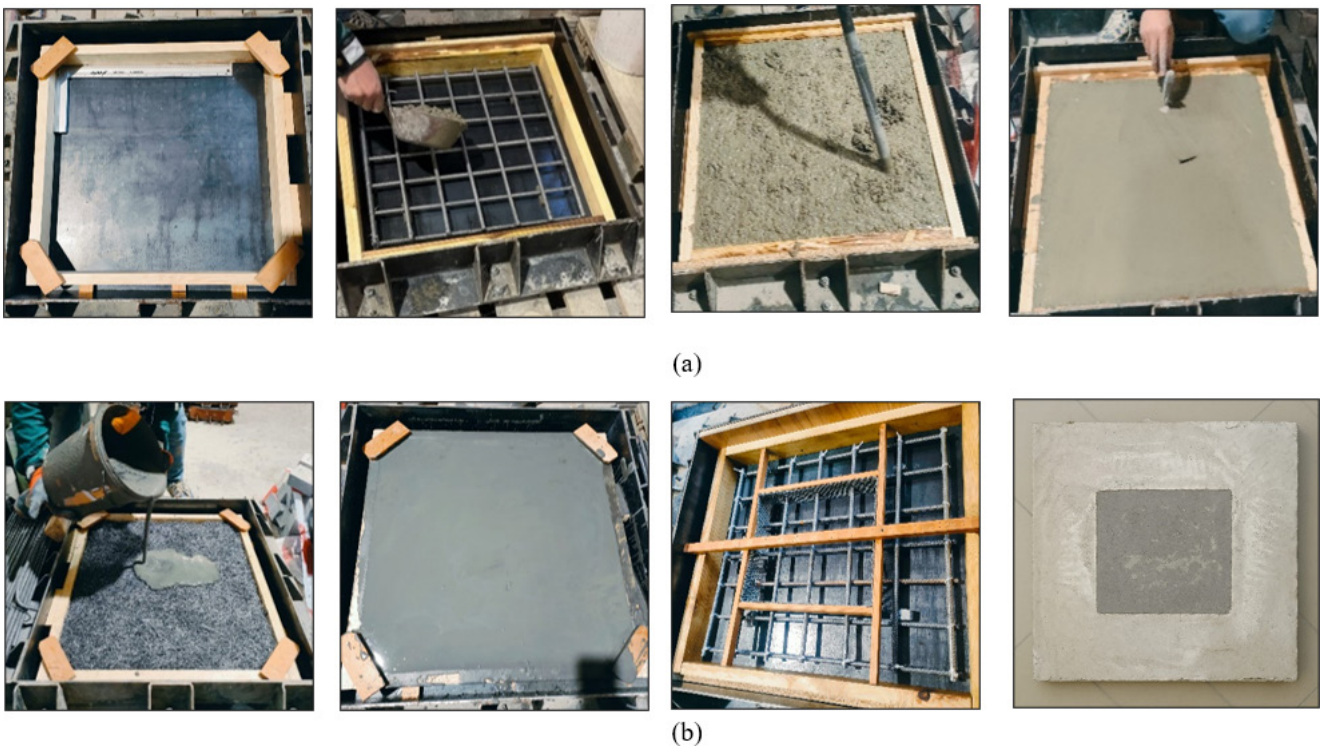


**Fig. 7** The steps of casting the different types of flat slab concrete: (a) NSC; (b) SIFCON and RC-SIFCON

using a calibrated electrical testing machine with a maximum range capacity of 500 kN as shown in Fig. 8. The load was applied gradually until failure occurred. Each slab was simply supported at the four edges with an equal span length of 500 mm, with the use of a special supporting frame that was manufactured and used inside the testing machine. This supporting frame was made using four steel beams welded and arranged to form a square shape.

The load was applied through a 60 × 60 mm steel stub column connected to the electrical testing machine actuator hung from a steel reaction frame. All specimens were tested at a constant loading rate of 0.5 mm/min. Linear variable differential transducers (LVDTs) were instrumented at the middle point and two opposite quarters of the slab span on either side of the load center to measure the slab deflection. This amount of incremental loading allowed for a sufficient number of load readings and corresponding deflections to be taken during the test, which gave a good picture of the structural behavior of the slab. The load at first crack, the ultimate punching shear or bending load, corresponding deflections at the slab center, and the deflection average of two quarters were all observed and recorded. The ultimate deflection is defined as the deflection corresponding to a reduction of the applied load to 80% of its peak value [15]. Given the focus of this study on high-ductility SIFCON, a detailed assessment of the post-peak response was undertaken to elucidate the fiber behavior under advanced deformation stages. Two distinct ultimate deflection points were identified beyond the peak load, corresponding to 80% and 60% of the peak load, respectively. Throughout this study, these points are denoted as $u_1$ (at 80% of the peak load) and $u_2$ (at 60% of the peak load).

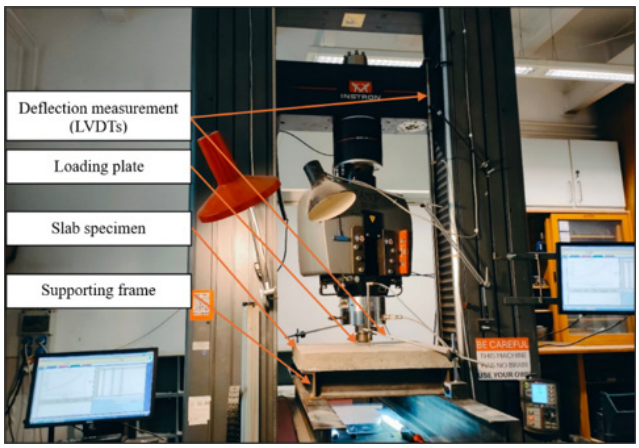


**Fig. 8** Punching shear test of slabs

## 3 Results and discussion

### 3.1 Mechanical properties

This study test the compressive strength and flexural strength of NSC and SIFCON concrete. The strength of compressive and flexural at the age of 7 and 28 days for the cubes and prisms prepared for this purpose was tested. Table 4 shows the results of the NSC and SIFCON. Logically, the results show that the compressive and flexural tensile strength of SIFCON is much higher than that of NSC. SIFCON contains a large amount of fiber, in this study, hook-end steel fiber was used. The enhancement in strength can explain the fibers' ability to restrict and prevent fracture expansion, as well as minimize crack growth rate and direction. The reason for increasing the strength is the possibility of expanding the steel fiber with a higher volume fraction value because it has high tensile strength, which causes a decrease in the crack amounts and the width of the crack by acting as a bridge for the crack in the sides, which is due to the growing strength.

### 3.2 First cracking strength

The main objective of this study is to know the behavior of RC flat slab when the SIFCON is used partially, including first crack, maximum load, deflection, and rotation, as well as the crack pattern of each specimen and the inclination of cracks. The first crack loads, for the various slabs, are summarized in Table 5. Also, Table 5 shows deflection of the center and the average deflection of two quarters at the first crack.

The results show that using SIFCON increased the first crack strength of the slab. The first crack strength increased with the area and depth of SIFCON. This is because the stiffness of the slabs increases with the area and depth of SIFCON. As the SIFCON area is increasing, a higher load is needed to crack the slab. The first crack load for the slab N-SC18-2, with SIFCON dimension 180 × 180 × 20 mm, increased by about 46% compared to the reference slab made entirely of NSC. The percentage increases shown in Table 5 and Fig. 9 were progressively greater with an increase in

**Table 4** The mechanical properties results of the NSC and SIFCON

| Type of concrete | Compressive strength (MPa) | | Flexural strength (MPa) | | The percentage increases (%) in 28 days compared to NSC | |
|---|---|---|---|---|---|---|
| | 7 days | 28 days | 7 days | 28 days | Compressive strength | Flexural strength |
| NSC | 31 | 43 | 3.7 | 4.8 | – | – |
| SIFCON | 89 | 118 | 23.5 | 32 | 174 | 567 |

**Table 5** The first crack load and deflection of the specimens

| Specimen | $P_{cr}$ (kN) | $\Delta_{cf}$ (mm) | $\Delta_{qf}$ (mm) | $\eta_f$ (%) |
|---|---|---|---|---|
| N | 11.18 | 1.23 | 0.21 | – |
| S | 49.43 | 2.82 | 2.35 | 342 |
| N-ST60-2 | 45.02 | 2.66 | 2.21 | 303 |
| N-ST60-4 | 47.69 | 2.54 | 1.84 | 327 |
| N-SC18-2 | 16.31 | 1.36 | 0.26 | 46 |
| N-SC18-4 | 20.13 | 2.14 | 1.09 | 80 |
| N-SC18-6 | 22.05 | 2.35 | 1.41 | 97 |
| N-SC30-6 | 23.80 | 2.47 | 1.53 | 113 |

In Table 5 $P_{cr}$ is the first cracking load; $\eta_f$ is the percentage of improved first crack strength compared to specimen N; $\Delta_{cf}$ is the center deflection at first cracking load; $\Delta_{qf}$ is the quarters av. deflection at first cracking load.

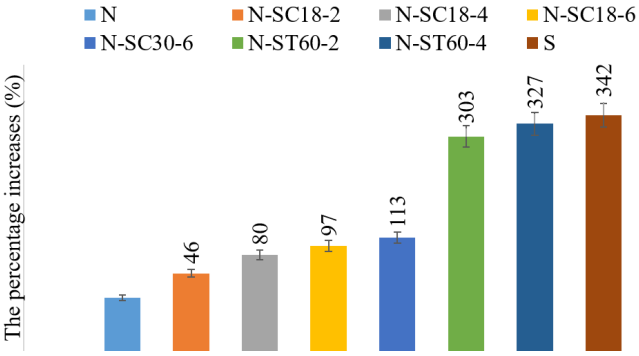


**Fig. 9** The percentage of improved first crack strength compared to specimen N

area or depth of SIFCON area or depth. On the other hand, the positive effect of the area of the SIFCON on the increase of cracking load was greater than the effect of the increase in depth. As full-depth SIFCON was used, with a SIFCON area of 180 × 180 mm, there was a limited increase (up to 97%) of the first crack strength. However, as a SIFCON of 600 × 600 mm was used, even with a SIFCON depth of only 20 mm, the first crack strength was increased by up to 303%. It should be noted that when using SIFCON in a partial area, the first crack begins at the dividing line between the SIFCON and the NSC.

### 3.3 Failure mode and crack pattern

Fig. 10 shows the crack distribution at the tension side of each tested specimen. Three different failure modes were observed in the tested specimen:

1. punching shear failure;
2. flexural failure;
3. combined punching shear-flexural failure.

Group 1 of specimens, N and S exhibits a punching shear failure and combined punching shear-flexural failure respectively. The load at the first crack of the N slab was

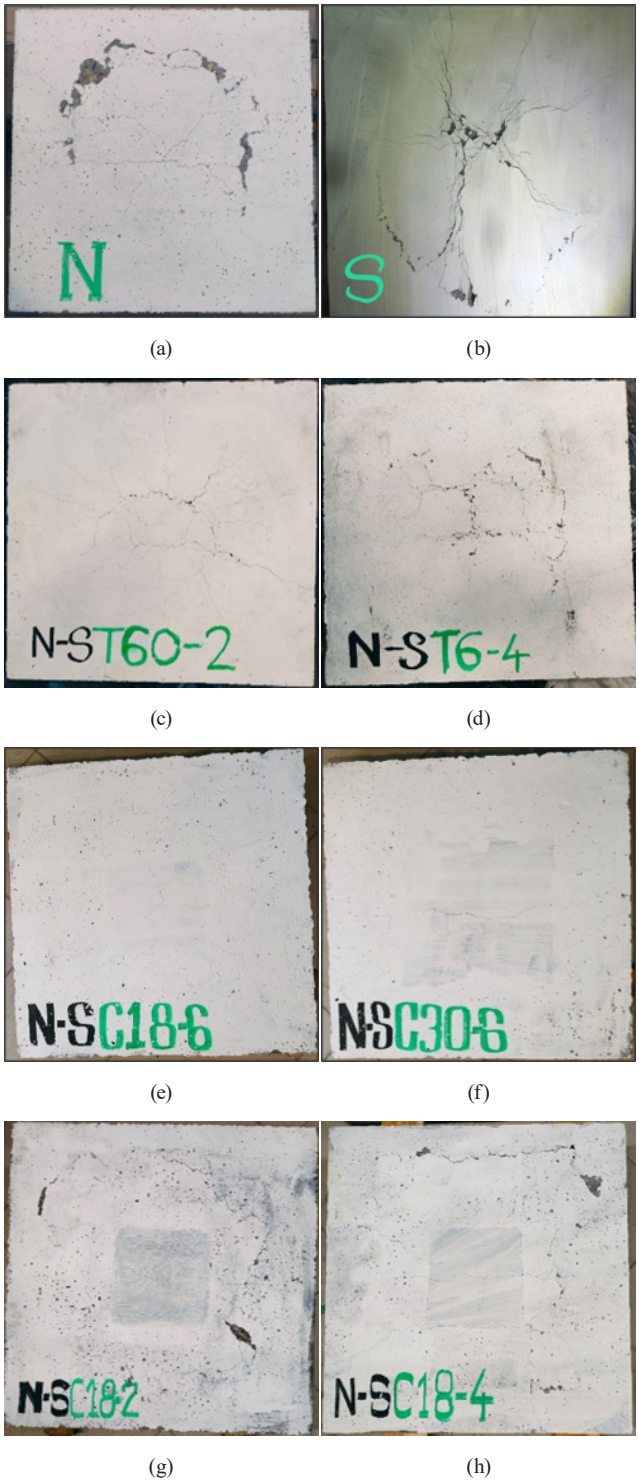


**Fig. 10** Crack patterns on tension sides and midspan cross sections: (a) Specimen N; (b) Specimen S; (c) Specimen N-ST60-2; (d) Specimen N-ST60-4; (e) Specimen N-SC18-2; (f) Specimen N-SC18-4; (g) Specimen N-SC18-6; (h) Specimen N-SC30-6

11.18 kN and 49.43 kN for the S slab. The cracks started from the area directly under the load until they formed a circular shape outside the perimeter of the load area for the N slab and diagonal cracks for the S slab and formed

a circular shape crack in the last, upon reaching the highest loads of 50.3 and 109.3 KN, where the deflection was 4.82 and 12.06 mm. It is worth noting that for the N slab, some parts of the concrete collapsed and spalled.

No significant readings were recorded for the $u_1$ and $u_2$ stages for the reference N slab, meaning that no high ductile behavior was observed for this slab. While for the slab S made entirely of SIFCON, the center deflection value was about 16.7 and 24.8 mm for $u_1$ and $u_2$, respectively. This indicates the high ductility of this slab due to the amount of fibers present, which led to it being able to bear high loads in the later stages.

Group 2 of specimens, N-ST60-2, exhibits a combined punching shear-flexural failure, while the failure for N-ST60-4 was punching shear failure. As the applied loading increased, the cracks formed with direction parallel to the reinforcement in the center of the slab. At peak load, the center deflections were approximately 5.5 and 8.7 mm for the N-ST60-2 and N-ST60-4 slabs, respectively. The maximum load for the N-ST60-4 was higher than the N-ST60-2 slab. Although the deflection at peak load to $u_1$ deflection was greater for slab N-ST60-4, it is noteworthy that slab N-ST60-2 exhibited a significantly larger difference in deflection during the continuous phase between $u_1$ and $u_2$. This resulted in more pronounced ductile behavior. The increase in deflection between $u_1$ and $u_2$ was measured at 5.8 mm for slab N-ST60-2 and only 2 mm for slab N-ST60-4. Nevertheless, the final deflection recorded at for $u_2$ was higher for slab N-ST60-4, reaching 13.5 mm.

Finally, Group 3 of specimens, N-SC18-2, N-SC18-4, N-SC18-6, and N-SC30-6, the failure mechanism was a combined punching shear-flexural failure, and the reaction was ductile load deflection. The first crack starts at the dividing line between the SIFCON and the NSC, continues around the SIFCON, and extends beyond this perimeter. As the load increases, very small cracks begin to appear in the SIFCON area and large ones outside this area, until the maximum load is reached, where the cone of the punching cracks is completed.

It is noted that in Group 3, the punching shear cracks are farthest from the critical punching area. The thicker the SIFCON or the area increases, the punching shear boundaries are almost adjacent to the external supports. The maximum load reached 62.91 kN for the N-SC30-6 slab, corresponding to the deflection of 6.53 mm. It is noted for the slabs of Group 3w in periods $u_1$ and $u_2$ that the difference in deflection increases with the gradual increase in the area or depth of the SIFCON. But it becomes clear that the ductility increases with the increase in the area, more than with the increase in the depth of the SIFCON used in the slab.

### 3.4 Peak load and load-deflection response

Table 6 and Fig. 11 presents the results of the peak loads (maximum loads) and corresponding deflections for the tested specimens, along with the percentage increase in maximum load compared to the reference specimen (N). Fig. 12 illustrate the load–deflection curves. The results demonstrate that increasing the area or depth of the SIFCON layer within the slab leads to an increase in the maximum load capacity. Slab S was the most improved in terms of peak load, with an increase of 117% compared to the maximum load of slab N. For composite (RC-SIFCON) flat slabs, the highest peak load development was in slab N-ST60-4, where the increase compared to slab N was about 112%. Notably, even in cases where the improvement in load capacity was relatively minor, such as in slabs incorporating a small volume of SIFCON concrete, a significant transformation in failure mode from brittle to ductile was observed.

**Table 6** The peak load and deflection of the specimens at the peak cracks

| Specimen | $P_p$ | $\Delta_{cp}$ | $\Delta_{qp}$ | $\eta_p$ |
|---|---|---|---|---|
| N | 50.18 | 4.82 | 2.25 | – |
| S | 109.3 | 12.06 | 5.25 | 117 |
| N-ST60-2 | 72.43 | 5.54 | 3.83 | 44 |
| N-ST60-4 | 106.26 | 8.71 | 4.06 | 112 |
| N-SC18-2 | 52.62 | 5.01 | 2.36 | 5 |
| N-SC18-4 | 54.02 | 6.03 | 2.45 | 8 |
| N-SC18-6 | 59.30 | 6.30 | 2.54 | 18 |
| N-SC30-6 | 62.91 | 6.53 | 2.62 | 25 |

In Table 6 $P_p$ is the Peak load (kN); $\Delta_{cp}$ and $\Delta_{qp}$ are the centers and quarters av. deflection (mm) at peak load, respectively; $\eta_p$ is the percentage of improved peak load compared to specimen N.

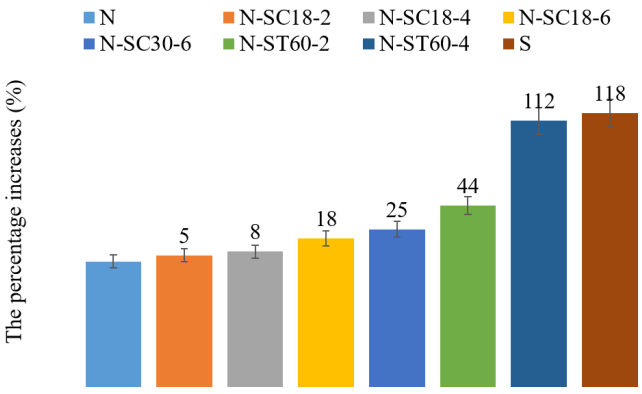


**Fig. 11** The percentage of improved maximum load compared to specimen N

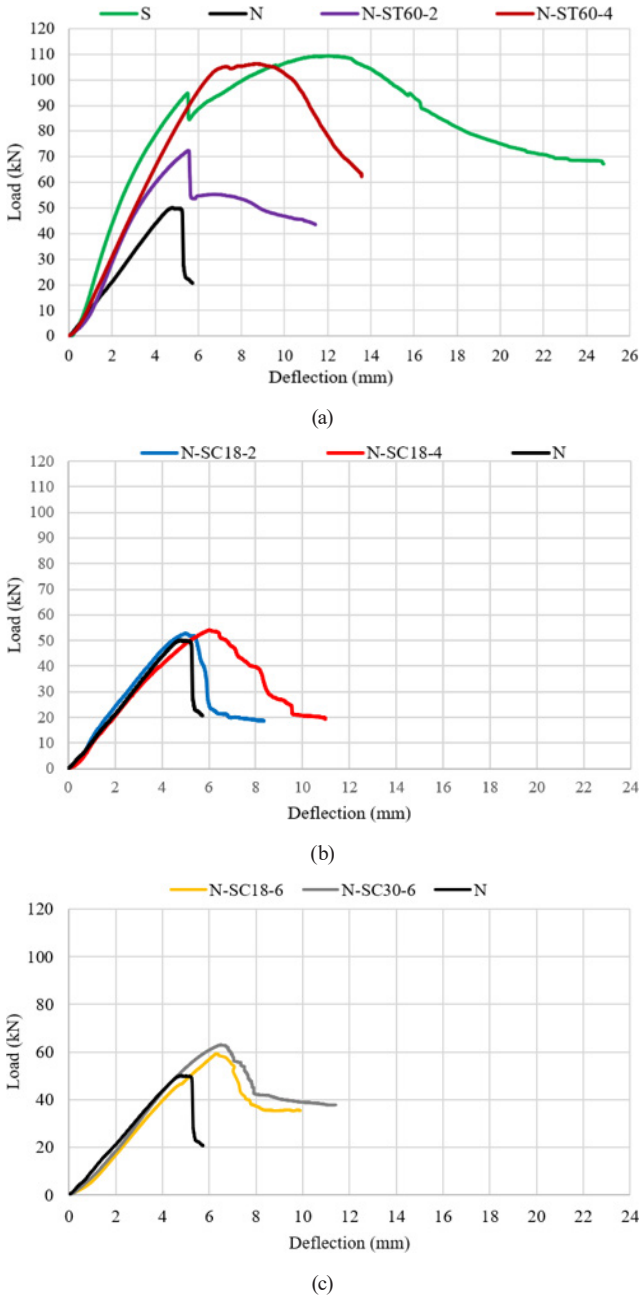


**Fig. 12** The load–center deflection curves: (a) Specimen N, S, N-ST60-2, and N-ST60-4; (b) Specimen N, N-SC18-2, and N-SC18-4; (c) Specimen N, N-SC18-6, and N-SC30-6

It was also noted that the difference in deflection $u_1$ and $u_2$ gradually increased with the increase in area or depth of SIFCON, with the area having a more pronounced effect. The most effective use of SIFCON was achieved by increasing the area, as this promoted a shift in the failure mechanism from punching shear to flexural failure, resulting in significantly enhanced ductility, as observed in specimens N-ST60-2 and N-ST60-4.

Among Group 3, slab N-SC30-6 demonstrated the highest peak load and deflection, attributed to its larger SIFCON area compared to the other slabs. The flat slab with SIFCON of the area of 180 × 180 mm, with part-depth, did not significantly enhance the shear capacity compared with the NC slab. In contrast, specimens N-SC18-2, and N-SC18-4, which shared the same SIFCON area but differed in overall depth, exhibited a shift in behavior during the later stages of loading after $u_1$ and $u_2$ for example 40% of maximum load as shown in Fig. 12 (b). For specimens N-SC18-6 and N-SC30-6, which have different areas but the same depth, the segment between points $u_1$ and $u_2$ exhibited a bigger difference in deflection, characterized by a noticeably gentle slope that was nearly parallel to the X-axis, indicating a plateau-like post-peak response that indicates ductile behavior, where the slab sustains large deflections with little reduction in load, as shown in Fig. 12 (c). This is due to the presence of large quantities of fibers that bridged the main cracks and transformed them into smaller sub-cracks, thus increasing the ductility. According to the *fib* Model Code for Concrete Structures 2010 [16], steel fibers contribute significantly to crack bridging and stress redistribution in FRC, especially in highly redundant structures like slabs. This effect enhances the structural ductility and controls the crack width even after cracking has initiated. This observation is particularly significant for flat slab systems, as it highlights the potential of SIFCON to improve ductility and reduce the risk of sudden failure. Such improvements can be achieved using relatively small amounts of SIFCON in terms of area and depth, eliminating the need to increase slab thickness or to use drop panels or column capitals.

The load-displacement curve of the S slab (green curve) in Fig. 12 (a) showed a slight drop in capacity following the initiation and propagation of punching shear cracks. This temporary reduction was subsequently compensated for by a gradual recovery, primarily due to the bridging and pull-out action of the steel fibers across the cracks. Cheng et al. similarly emphasized that steel fibers enhance the post-cracking response and residual strength of slabs subjected to punching shear [17].

### 3.5 Ductility

The ductility ($\mu$) is defined as the ability of the structure or parts of it to sustain large deformations beyond the yield point, which is obtained in terms of displacements, as the ultimate displacement ($\Delta u$) divided by the yield displacement ($\Delta y$). The ductility index ($\mu$) had been calculated using Eq. (1), as suggested in Lim and Hong [18]. The ultimate displacement at failure is defined as the deflection when

the load drops to 80% of the peak load. The secant stiffness at a point two-thirds of the measured peak strength is used to idealize the elastoplastic curve that passes through the peak point of the load-displacement curve, and the displacement at an intersecting point between the two lines is used to determine the yield point on the curve [14, 18, 19]. The ductility ($\mu_1$ and $\mu_2$) was found to be assuming the ultimate deflection at two stages ($u_1$ and $u_2$), to more accurately understand the behavior of the slabs and the performance of the fibers at these later periods. All results are listed in Table 7.

$$\mu = \frac{\Delta u}{\Delta y} \tag{1}$$

Table 7 and Fig. 13 reveals a significant enhancement in ductility with the incorporation of SIFCON in the slab. In the first stage ($u_1$), which occurs after the peak load, ductility improves progressively. A significant improvement was observed for the second stage ($u_2$). Notably, for RC-SIFCON slab, a considerable improvement is observed during the transitional phase between these two stages when a uniform 2 cm SIFCON layer is applied across the entire slab surface like for N-ST60-2 slab. This can be attributed to the fact that, once the reinforcing steel reaches its full yield, the fiber begin to engage in resisting the applied loads by bridging cracks and minimizing their size. This mechanism allows the structure to maintain its load-carrying capacity for a longer duration, effectively shifting the failure mode from brittle to ductile. This outcome fulfills the primary objective of the study, demonstrating that excellent ductility can be achieved with a relatively small amount of SIFCON.

**Table 7** The ductility results

| Specimen | $P_y$ | $\Delta cy$ | $\Delta cu_1$ | $\Delta cu_2$ | $\mu_1$ | $\mu_2$ | $\eta\mu_1$ | $\eta\mu_2$ |
|---|---|---|---|---|---|---|---|---|
| N | 48.90 | 4.65 | 5.22 | 5.30 | 1.12 | 1.14 | – | – |
| S | 93.94 | 5.40 | 16.70 | 24.80 | 3.09 | 4.59 | 176 | 302 |
| N-ST60-2 | 65.73 | 4.63 | 6.74 | 11.43 | 1.46 | 2.47 | 30 | 117 |
| N-ST60-4 | 100.69 | 6.45 | 11.49 | 13.50 | 1.78 | 2.09 | 59 | 83 |
| N-SC18-2 | 49.97 | 4.46 | 5.66 | 5.93 | 1.27 | 1.33 | 13 | 17 |
| N-SC18-4 | 49.93 | 5.16 | 7.12 | 8.39 | 1.31 | 1.64 | 17 | 44 |
| N-SC18-6 | 56.71 | 5.21 | 7.22 | 9.91 | 1.39 | 1.90 | 24 | 67 |
| N-SC30-6 | 59.84 | 5.36 | 7.63 | 10.89 | 1.42 | 2.03 | 27 | 78 |

In Table 7 $P_y$ is the yield load (kN); $\Delta cy$ is the center deflection (mm) at yield load; $\Delta cu_1$ and $\Delta cu_2$ are the center ultimate deflections (mm) of $u_1$ and $u_2$, respectively; $\mu_1$ and $\mu_2$ are the ductilities 1 and 2; $\eta\mu_1$ and $\eta\mu_2$ are the percentages of improved ductility 1 and 2 compared to specimen N.

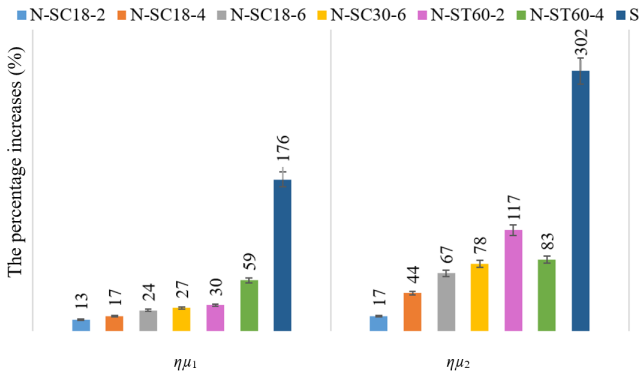


**Fig. 13** The percentage of improved ductility compared to specimen N

### 3.6 Inclination of cracks and rotation of slabs

Following the slab tests' completion, the slabs' rotation angle around the loading zone was measured. Several slabs were then cut in half to examine the principal crack orientations, as presented in Fig. 14, where the specimens in Groups 1 and 2 were cut to observe the effect of using SIFCON depth gradually. By identifying the cracks formed on both the slabs' top and bottom surfaces, the punching cone's failure angle was determined as the angle between the failure surface and the vertical plane. It was noted that the angle between the cracks and the horizontal axis on the tension side decreased with increasing SIFCON depth in the slab. This observation indicates that the primary cracks gradually shifted away from the critical punching shear zone, leading to a transition in the failure mechanism from brittle to ductile. Additionally, the slab rotation angle increased with the use of SIFCON, particularly when a larger SIFCON area was incorporated.

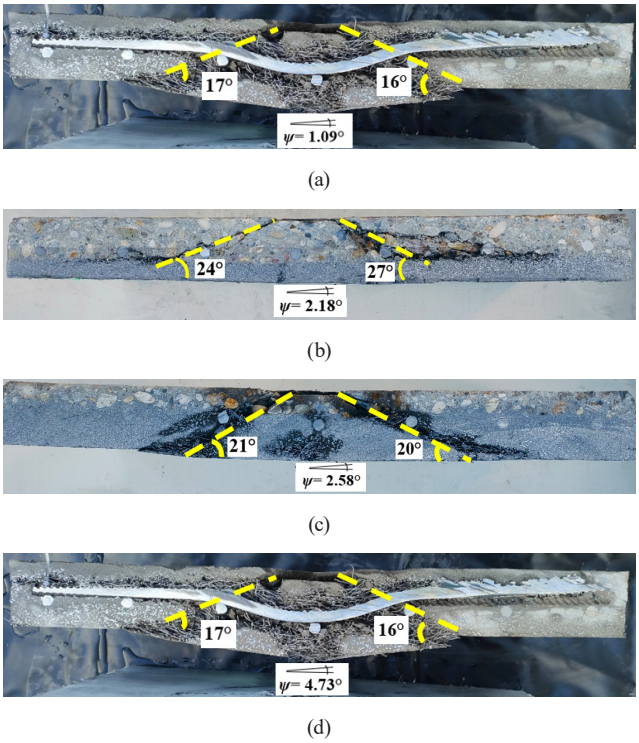


**Fig. 14** Inclination of cracks and rotation of slabs: (a) Specimen N; (b) Specimen N-ST60-2; (c) Specimen N-ST60-4; (d) Specimen S

The experimental results align with the consensus that the punching behavior of a flat slab is governed by the development and rotation of a critical shear crack. In systems incorporating high fiber contents such as SIFCON, fiber bridging across inclined cracks enhance post-cracking tensile, which delays crack localization and improves the punching resistance. In our tests, SIFCON and RC-SIFCON hybrid specimens exhibited higher peak capacity, and a more gradual post-peak response compared to normal RC specimen, indicating a shift from brittle punching toward a more ductile flexure-punching mechanism. These results agree with prior research [17] on fiber and support the idea that fiber volume fraction and concrete strength are key levers for controlling punching strength and deformation capacity.

Previous studies have indicated beneficial effects of fibers on shear strength; however, data sets on RC-SIFCON hybrid slabs remain comparatively scarce. The present study addresses part of this gap by providing controlled experimental evidence on SIFCON and RC-SICON flat slabs under punching and by discussing the influence on deformation capacity and failure mode.

## 4 Conclusions

The present study investigates the mechanical properties of SIFCON incorporating 6% hooked-end steel fibers and evaluates the structural performance of RC flat slabs partially using SIFCON. The research specifically directed to the punching shear resistance of RC-SIFCON flat slabs. The experimental results are presented, including the compressive and flexural strength characteristics of the SIFCON and NSC, maximum load, deflection, ductility, and rotation, as well as the crack pattern of each specimen and the inclination of cracks. The findings of this study contribute to a deeper understanding of the structural behavior and enhancement potential of hybrid RC-SIFCON systems under punching shear loading. The conclusions highlighted and documented the most significant findings and insights derived from the study, emphasizing their scientific relevance and potential implications for future research and practical applications:

1. *The mechanical properties* of the two types of concrete used in this study, SIFCON and NSC, were assessed at 7 and 28 days. The compressive strength at 28 days reached 118 and 43 MPa on average for SIFCON and NSC, respectively. Similarly, the flexural strength of SIFCON was 32, while NSC recorded only 4.8 MPa. These results reveal a significant difference between the two mixes, with SIFCON demonstrating superior mechanical behavior characteristic of high-performance concrete. This confirms the intended functional roles, where SIFCON acts as the strengthening material and NSC serves as the base or reference concrete.
2. *The first cracking load* showed a clear improvement in the slabs with SIFCON. The SIFCON slab shows the greatest increase, with a 342% improvement over the NSC slab control. RC-SIFCON slabs, which combine SIFCON and NSC, also exhibited significant improvement, with an increase of 46–327%, but NSC slabs had the lowest resistance to early cracking. These results highlight the major function of SIFCON in delaying the growth of cracks. Compared to NSC, the higher first cracking load observed in SIFCON slabs is primarily attributed by the dense distribution of steel fibers. These fibers enhance the material's tensile strength, effectively bridge microcracks, and delay crack initiation, thereby enabling the slab to sustain greater loads before the appearance of visible cracks.
3. *The maximum load bearing capacity* showed substantial improvement in the SIFCON-strengthened slab compared to the conventional NSC slab. The SIFCON slab exhibited the highest enhancement, with an increase of 117% relative to the control. RC-SIFCON slabs in the Group 2 also made significant gains, with improvements of 44% and 112%, depending on the SIFCON configuration. Group 3 of slabs showed noticeable improvement, with improvements ranging from 5–25%, depending on the SIFCON depth and area. In contrast, the NSC slab maintained the lowest ultimate load. These findings confirm the high structural efficiency of SIFCON, particularly in enhancing load-bearing capacity under extreme conditions. These findings highlight the potential of SIFCON as an effective solution for strengthening flat slabs, particularly in structures exposed to high service loads.
4. *The load–deflection curves* showed that the SIFCON slab had a gradual post-peak decline, indicating high ductility, unlike the NSC slab, which failed sharply. RC-SIFCON Group 2 showed a smoother descent than NSC, while Group 3 maintained after 80% of the peak load, dropping with moderate softening. Ultimate deflections reached (SIFCON: 24.8 mm, Group 2: 13.5 mm, Group 3: 10.9 mm, and NSC: 5.3 mm), highlighting the superior deformability of SIFCON and the improved behavior of hybrid slabs.

5. *The failure modes* varied significantly among the tested slabs. NSC slabs exhibited brittle punching shear failure with wide, steep cracks forming at angles of approximately 32°, indicating low ductility. In contrast, SIFCON slabs failed in a ductile manner with multiple fine cracks spreading at angles around 17°, reflecting enhanced crack resistance. Hybrid slabs showed mixed behavior; Groups 2 and 3 had more distributed cracks with moderate angles (20°–27°), exhibited improved crack patterns compared to NSC, but less controlled than full SIFCON. Additionally, the slab rotation angle around the load area increased with the use of SIFCON, particularly when a larger SIFCON area was incorporated, reaching (4.73°) for S slab, indicating a shift toward a more ductile and distributed failure mode. This behavior reflects the ability of fibers to extend the crack path and enhance the energy absorption capacity before failure.
6. *Ductility* analysis showed a marked improvement in slabs incorporating SIFCON. The SIFCON slab demonstrated the highest ductility index, reflecting its superior energy absorption and deformation capacity before failure. RC-SIFCON slabs, especially Group 2, also showed enhanced ductility compared to NSC, though lower than full SIFCON. In contrast, the NSC slab exhibited the lowest ductility, failing in a sudden and brittle manner. For the first time, the ductility of late stages, at deflection $u_1$ and $u_2$, was studied to determine the behavior of fibers at these stages. The percentage increase in the last ductility $\eta\mu_2$ indices recorded was (SIFCON: 302%, Group 2: 117%, and Group 3: 78%) compared with NSC, confirming the role of SIFCON in enhancing structural resilience, this post-peak response highlights the enhanced energy absorption capacity of SIFCON, providing a safer and more resilient structural performance than conventional slabs.
7. Future research should extend the experimental program to include the effects of load eccentricity, edge and corner columns, as well as cyclic loading conditions. It is also recommended to investigate volume effects and different fiber type and ratios.

## References

[1] Isufi, B., Relvas, J. P., Marchão, C., Ramos, A. P. "Behavior of flat slabs with partial use of high-performance fiber reinforced concrete under monotonic vertical loading", Engineering Structures, 264, 114471, 2022. https://doi.org/10.1016/j.engstruct.2022.114471

[2] Halvoník, J., Kalická, J., Majtánová, L., Minárová, M. "Reliability of models aimed at evaluating the punching resistance of flat slabs without transverse reinforcement", Engineering Structures, 188, pp. 627–636, 2019. https://doi.org/10.1016/j.engstruct.2019.03.055

[3] Saleh, H., Kalfat, R., Abdouka, K., Al-Mahaidi, R. "Punching shear strengthening of RC slabs using L-CFRP laminates", Engineering Structures, 194, pp. 274–289, 2019. https://doi.org/10.1016/j.engstruct.2019.05.050

[4] Tahmoorian, F., Nemati, S., Sharafi, P., Samali, B., Khakpour, S. "Punching behavior of foam-filled modular sandwich panels with high-density polyethylene skins", Journal of Building Engineering, 33, 101634, 2021. https://doi.org/10.1016/j.jobe.2020.101634

[5] Yehia, E., Hussein Khalil, A., Mostafa, E.-E., Abdelfattah El-Nazzer, M. "Experimental and numerical investigation on punching behavior of ultra-high performance concrete flat slabs", Ain Shams Engineering Journal, 14(10), 102208, 2023. https://doi.org/10.1016/j.asej.2023.102208

[6] Facconi, L., Minelli, F., Plizzari, G. "Steel fiber reinforced self-compacting concrete thin slabs – Experimental study and verification against Model Code 2010 provisions", Engineering Structures, 122, pp. 226–237, 2016. https://doi.org/10.1016/j.engstruct.2016.04.030

[7] Nguyen-Minh, L., Rovňák, M., Tran-Quoc, T., Nguyenkim, K. "Punching Shear Resistance of Steel Fiber Reinforced Concrete Flat Slabs", Procedia Engineering, 14, pp. 1830–1837, 2011. https://doi.org/10.1016/j.proeng.2011.07.230

[8] Ipek, M., Aksu, M. "The effect of different types of fiber on flexure strength and fracture toughness in SIFCON", Construction and Building Materials, 214, pp. 207–218, 2019. https://doi.org/10.1016/j.conbuildmat.2019.04.055

[9] Tauma, W. K., Balázs, G. L. "Impact and blast resistance of slurry infiltrated fiber concrete (SIFCON): A comprehensive review", Concrete Structures, 24, pp. 129–136, 2023. https://doi.org/10.32970/CS.2023.1.18

[10] ASTM International "ASTM C1240-15 Standard Specification for Silica Fume Used in Cementitious Mixtures", ASTM International, West Conshohocken, PAUSA, 2015. https://doi.org/10.1520/C1240-15

[11] ASTM International "ASTM C494/C494M-15 Standard Specification for Chemical Admixtures for Concrete", ASTM International, West Conshohocken, PA, USA, 2015. https://doi.org/10.1520/C0494_C0494M-15

[12] ACI "ACI 318-19 Building Code Requirements for Structural Concrete", American Concrete Institute, Farmington Hills, MI, USA, 2019.

[13] ASTM International "ASTM C1437-15 Standard Test Method for Flow of Hydraulic Cement Mortar", ASTM International, West Conshohocken, PA, USA, 2015. https://doi.org/10.1520/C1437-15

[14] BSI "BS EN 1992-1-1 Eurocode 2: Design of concrete structures – Part 1-1: General rules and rules for buildings", British Standards Institution, London, UK, 2004.

[15] Kaka, V. B., Kim, J., Chao, S.-H. "Formulating Constitutive Stress-Strain Relations for Flexural Design of Ultra-High-Performance Fiber-Reinforced Concrete", In: Proceedings of the First International Interactive Symposium on UHPC, Des Moines, IA, USA, 2016, pp. 1–10. ISBN 978-2-35158-164-3 [online] Available at: https://www.extension.iastate.edu/registration/events/UHPCPapers/UHPC_ID46.pdf [Accessed: 27 June 2025]

[16] *fib* "*fib* Model Code for Concrete Structures 2010", Ernst & Sohn, 2013. ISBN 978-3-433-60408-3 [online] Available at: https://content.e-bookshelf.de/media/reading/L-4005991-4171779882.pdf [Accessed: 27 June 2025]

[17] Cheng, C., Taffese, W. Z., Hu, T. "Accurate Prediction of Punching Shear Strength of Steel Fiber-Reinforced Concrete Slabs: A Machine Learning Approach with Data Augmentation and Explainability", Buildings, 14(5), 1223, 2024. https://doi.org/10.3390/buildings14051223

[18] Lim, W.-Y., Hong, S.-G. "Shear Tests for Ultra-High Performance Fiber Reinforced Concrete (UHPFRC) Beams with Shear Reinforcement", International Journal of Concrete Structures and Materials, 10(2), pp. 177–188, 2016. https://doi.org/10.1007/s40069-016-0145-8

[19] Sukontasukkul, P., Nimityongskul, P., Mindess, S. "Effect of loading rate on damage of concrete", Cement and Concrete Research, 34(11), pp. 2127–2134, 2004. https://doi.org/10.1016/j.cemconres.2004.03.022